

A reversion of atomic segregation under ion bombardment of Ni_xPd_y alloys

V.S. Chernysh^a, A.S. Patrakeeve^b and V.I. Shulga^{b*}

^a*Faculty of Physics, Moscow State University, Moscow, Russia;* ^b*Institute of Nuclear Physics, Moscow State University, Moscow, Russia*

(Received 20 July 2007; final version received 9 August 2007)

The angular distribution of atoms sputtered from Ni_xPd_y alloys ($x, y = 1, 5$) under 3 and 10 keV Ar⁺ ion bombardment has been studied experimentally and using computer simulations. A collector technique combined with RBS to analyze the distribution of collected material was used. It was found that the Pd/Ni yield ratio increases with the polar ejection angle θ for all targets excluding NiPd₅. This peculiarity of sputtering was explained by a reversion of atomic segregation at high initial concentrations of Pd atoms in the target.

Keywords: sputtering; angular distribution; surface segregation; NiPd alloys; experiment; computer simulation

1. Introduction

Ion bombardment of a solid material causes various phenomena, including sputtering of the target due to collisions of the incident ions with the target atoms and collision cascades between the target atoms. The collision process is more complicated for two- and multi-component targets, where different components may get different amount of energy from the bombarding ions and where the energy losses of light and heavy species during their motion in the target may be very different. This leads to the so-called preferential sputtering of light component during the initial stage of ion bombardment and to enrichment of the component with the lower sputtering yield on the surface under steady-state conditions (1).

Since the pioneering studies of Andersen et al. (2, 3), it is well known that the sputtering of two-component targets may be strongly affected by the ion-induced surface segregation of atoms. This is particularly true for the angular distribution of sputtered atoms, which is highly dependent on the state of the surface during ion bombardment. The surface segregation of one of the species changes the surface composition of atoms and leads to a pronounced angular dependence of the ratio of the partial sputtering yields.

*Corresponding author. Email: shulga@hep.sinp.msu.ru

Until now, the effect of surface segregation on the angular distribution of sputtered atoms was studied for a few target materials only, which does not allow to follow the influence of the initial concentration of the target elements. The purpose of the present research is to understand better the processes that control the sputtering of the targets with very different initial concentrations of components. The results show that at high initial concentrations of one of the components a reversion of atomic segregation is possible.

2. Experiment

The sputtering experiments were carried out using a UHV setup (4) consisting of a duoplasmatron ion source, electrostatic lenses and a magnetic separator for the primary beam and a sample chamber. The investigated targets were cut from the polycrystalline Ni₅Pd, Ni₃Pd, NiPd, NiPd₃ and NiPd₅ alloys with the average grain size less than 20 μm. The targets size was about 10 × 10 × 2 mm. X-ray diffraction analysis of the targets revealed an absence of the texture that could lead to some peculiarities of angular distributions of sputtered atoms. Before mounting to the experimental chamber, the samples were polished mechanically and then to degrease the surface were boiled in organic solvents. The target chamber was pumped down by a sorption roughing pump and a magnetic-discharge pump up to $2 \div 3 \times 10^{-6}$ Pa.

The irradiation was performed along the normal to the sample surface by mass separated Ar⁺ ions with energies 3 and 10 keV. The beam current density depending on the ion beam energy was $30 \div 400 \mu\text{A}/\text{cm}^2$. To reach the stationary regime of sputtering, the bombarding fluence was about 10^{18} ions/cm². The angular distributions of sputtered atoms were measured by using the collector technique. Sputtered material was deposited on a semi-cylindrical Al foil collector surrounded the target. The radius of the collector was 15 mm. The distribution of the sputtered material along the collector was measured by using RBS analysis with 1.5 MeV He⁺ ions. The resolution of the RBS measurements of angular distributions of sputtered atoms was $\pm 2^\circ$. The exposure to create the RBS spectrum was chosen to provide accuracy less than 5% for the emission angles $\theta > 70^\circ$, where the intensity of sputtering was low. To provide the sufficient reliability of results in case of NiPd₅ the collectors were investigated additionally by X-ray microanalysis. These measurements were done in the scanning electron microscope SEM LEO1455VP with a Roentek set-up for X-ray microanalysis. Secondary gamma radiation spectra were recorded in 1.5 mm discrete steps along the collector axis that corresponds to 5° steps of the emission angle.

3. Computer simulation

The simulations were performed using the computer code OKSANA (5). The code is based on the binary collision approximation and takes into account weak simultaneous collisions at large distances. The structure of the target is considered to be random (amorphous), as it is often assumed in calculations of sputtering of polycrystalline materials (6). As for amorphous Si and Ge targets (7), the target is simulated by rotation of a crystalline atomic block, the procedure of rotation being repeated from collision to collision. The standard WHB (KrC) potential is applied as the interaction potential for colliding particles (see (8)). The inelastic energy losses were calculated using the Firsov formula. Allowance was made for the uncorrelated thermal vibration in terms of the Debye model ($T = 300$ K). The surface potential barrier simulating the action of the long-range attractive force was planar. The atomic densities of elemental Ni and Pd targets differ by a factor of 1.3 ($N = 0.09126$ and 0.06767 atoms/Å³ for Ni and Pd, respectively), thus for Ni_xPd_y alloys the average value of density, which takes into account the actual concentrations of Ni and Pd atoms, was used. By analogy with ref. (9), the effective surface binding energy was calculated

in a similar way by the use of the heats of sublimation for elemental Ni and Pd targets ($U = 4.46$ and 3.91 eV, respectively). Note, however, that the variation of the surface binding energy in the range of $3.9\text{--}4.5$ eV has almost no impact on the simulated Pd/Ni yield ratios. A typical run consisted of about 3×10^6 sputtered atoms. All other parameters were identical to the standard model (10, 11).

To take into account composition changes in the Ni_xPd_y target due to preferential sputtering, the ratio of Pd and Ni concentrations, $C_{\text{Pd}}/C_{\text{Ni}}$, as a function of depth z was given by the linear

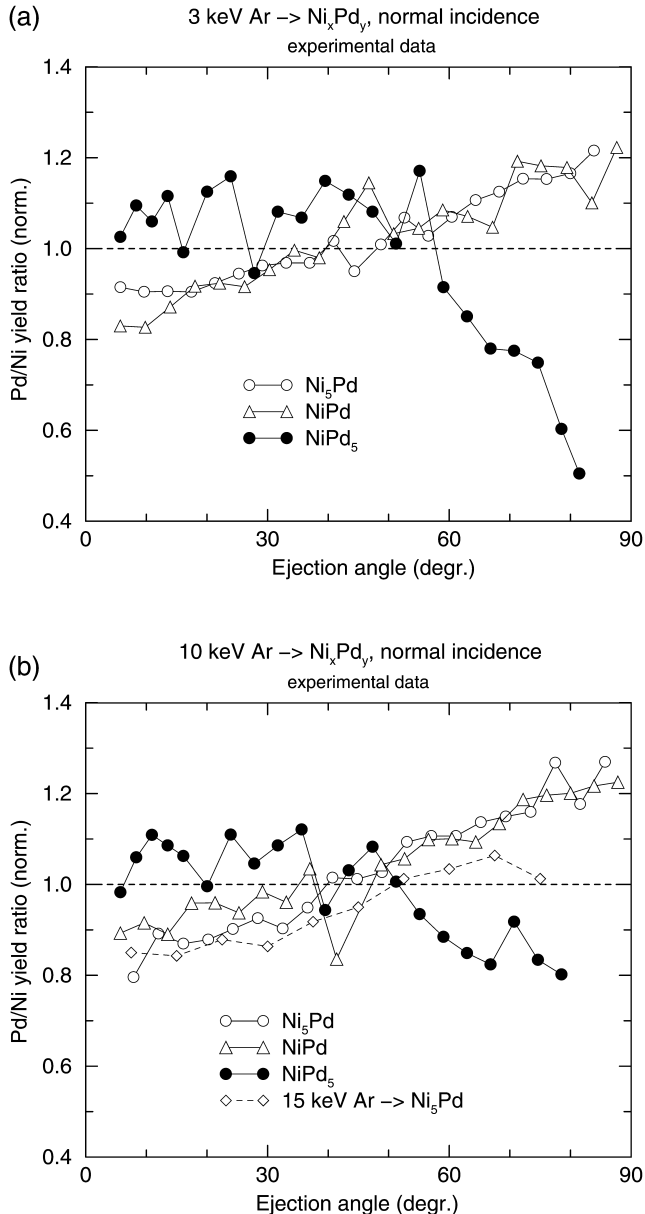


Figure 1. The angular dependences of the Pd/Ni yield ratio measured for different Ni_xPd_y targets bombarded with 3 keV (a) and 10 keV (b) Ar^+ ions at normal incidence. Also included are the experimental data for 15 keV Ar on Ni_5Pd (3).

dependence

$$C_{Pd}/C_{Ni} = [A - (A - 1)z/B]y/x \quad 0 \leq z \leq B$$

$$= y/x \quad z > B. \quad (1)$$

Here $z = 0$ corresponds to the target surface, B is the thickness of the altered layer, $B \approx 2R_p$, where R_p is the average projective range of ions. Equation (1) describes reasonably well the experimental concentration profiles (see Figure 5 in ref. (12)). In the case studied, $R_p \approx 25 \text{ \AA}$ and hence $B \approx 50 \text{ \AA}$. The fitting parameter A was found to satisfy the steady-state condition $Y_{Pd}/Y_{Ni} = y/x$, where Y_{Pd} and Y_{Ni} are the simulated values of the partial sputtering yields.

The above model does not take into account any effects of surface segregation of atoms. To simulate such effects, an extra monolayer of Ni and/or Pd adatoms was added at $z < 0$. The concentration of segregating adatoms, S_{Ni} and S_{Pd} , was prescribed. Simulation runs were performed with different values of A to find a new value of A at which $Y_{Pd}/Y_{Ni} = y/x$. Such simulations were repeated then at various concentrations of adatoms and the calculated angular dependences of the Pd/Ni yield ratio were compared with experimental data.

4. Results and discussion

The normalized angular dependences of the Pd/Ni yield ratio measured for three different Ni_xPd_y targets bombarded with 3 and 10 keV Ar ions are shown in Figure 1. Also shown (Figure 1 (b)) are the experimental data for a Ni_5Pd target bombarded with 15 keV Ar ions (3). It is seen that the results do not exhibit any pronounced dependence of the Pd/Ni yield ratio on the bombarding energy. The most striking feature is a very strong variation of the angular dependences of the yield ratio in going from Ni_5Pd and NiPd to $NiPd_5$. For a Ni_5Pd alloy, the increase of the Pd/Ni yield ratio with the polar ejection angle was explained (3) by surface segregation of Pd atoms. An

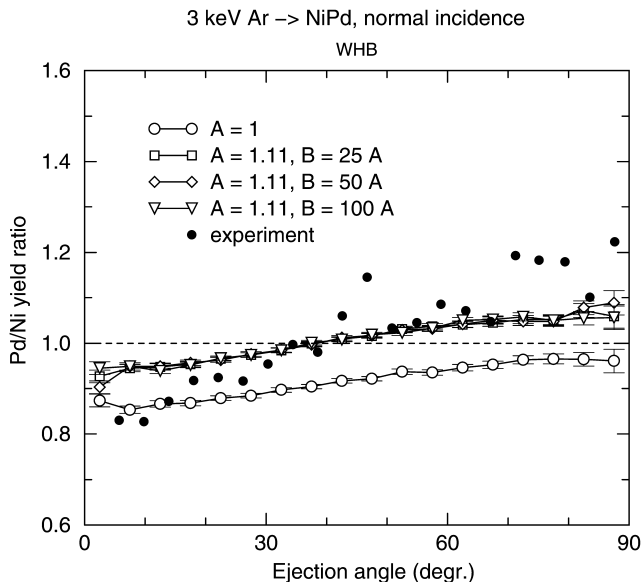


Figure 2. The angular dependences of the Pd/Ni yield ratio calculated at different values A and B in Equation (1) for a NiPd target bombarded with 3 keV Ar ions. The $A = 1$ curve corresponds to sputtering of a virgin target (low fluence, no surface segregation). Dots are the experimental data.

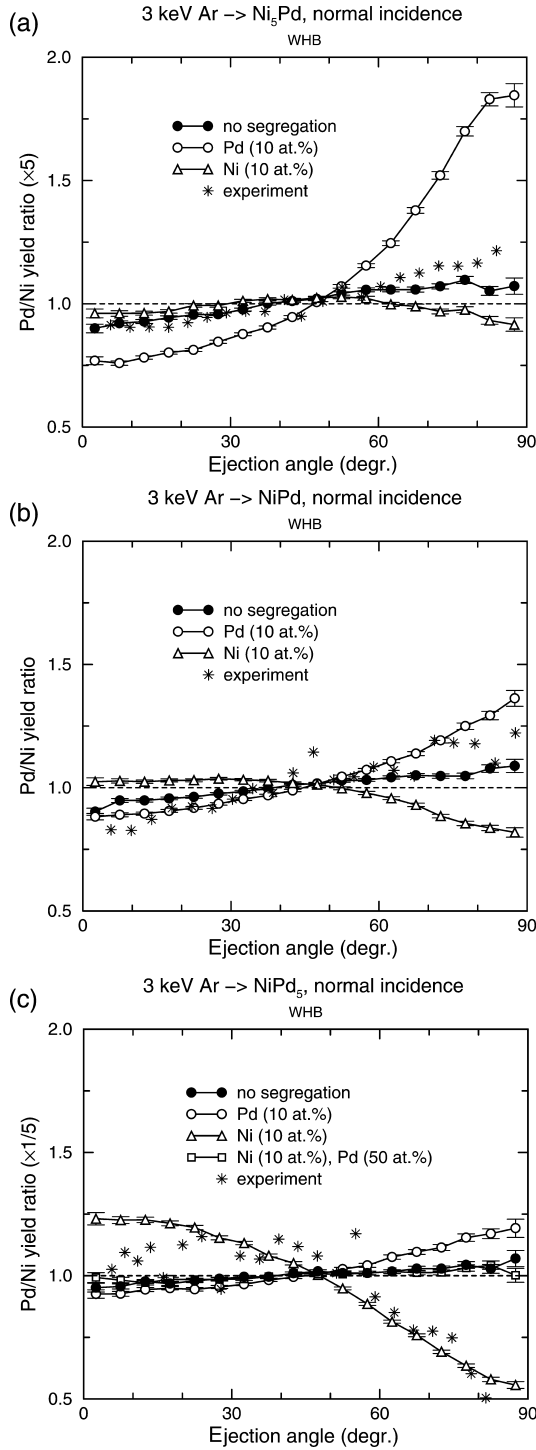


Figure 3. The angular dependences of the Pd/Ni yield ratio calculated for Ni₅Pd (a), NiPd (b) and NiPd₅ (c) targets bombarded with 3 keV Ar ions. Dots are the experimental data.

opposite behavior of the angular dependences (Figure 1) suggests that surface segregation of Ni is also possible. This happens in case when Ar ions bombard a NiPd₅ target, *i.e.* a target with a high bulk concentration of Pd.

Figure 2 presents the results of computer simulations referring to 3 keV Ar ions bombarding a NiPd target. The angular dependences shown were calculated at different values of the parameters A and B in Equation (1). At $A = 1$ no changes in the target composition were taken into account and, as a result, at all angles we have $Y_{Pd} < Y_{Ni}$. This is clear evidence for the effect of preferential sputtering. Three other dependences were calculated at $A = 1.11$ and various values of B . The value of $A = 1.11$ was found from the steady-state condition $Y_{Pd}/Y_{Ni} = 1$. One can see that the results are insensitive to B . This is important because the relevant function, Equation (1), is only a rough approximation of the depth dependence of C_{Pd}/C_{Ni} . From Figure 2 it is obvious that the effect of preferential sputtering alone is not enough to explain the results of measurements for a NiPd alloy, namely, a strong angular gradient of the Pd/Ni yield ratio.

Figure 3 presents more simulation data for the case of 3 keV Ar ion bombardment. The simulations were performed in three ways: (i) without any segregation; (ii) segregation of Pd; (iii) segregation of Ni. In order to estimate the significance of segregation, the concentrations of segregating atoms were taken to be identical, namely, $S_{Ni} = S_{Pd} = 10$ at.%. As above, in all cases the value of A in Equation (1) was varied to satisfy the condition $Y_{Pd}/Y_{Ni} = y/x$. It was assumed that $B = 50$ Å.

From Figure 3 it is seen that the effects of Pd and Ni segregation generally go into opposite directions. This is most evident for oblique ejection ($\theta > 60^\circ$), when $Y_{Pd}/Y_{Ni} > 1$ and $Y_{Pd}/Y_{Ni} < 1$ for Pd and Ni segregation, respectively. It is obvious that the value of $S_{Pd} = 10$ at.% greatly overestimates the effect of segregation for a Ni₅Pd alloy (Figure 3 (a)) but looks reasonable for a NiPd alloy (Figure 3 (b)). Note that in the latter case the relevant value of A was found to be 0.92. Quite a different situation is met for a NiPd₅ alloy (Figure 3 (c)), where the value of $S_{Ni} = 10$ at.% gives a good fit to the experimental data ($A = 2.3$). The reversion of atomic segregation (Ni instead of Pd) can be explained by a high near-surface concentration of Pd atoms, which try to get out of their foreign (and preferentially sputtered) Ni atom surroundings.

Figure 3 (c) also shows the results of simulations carried out for a top monolayer containing 10 at.% of Ni and 50 at.% of Pd, which corresponds to the proportion between Ni and Pd atoms

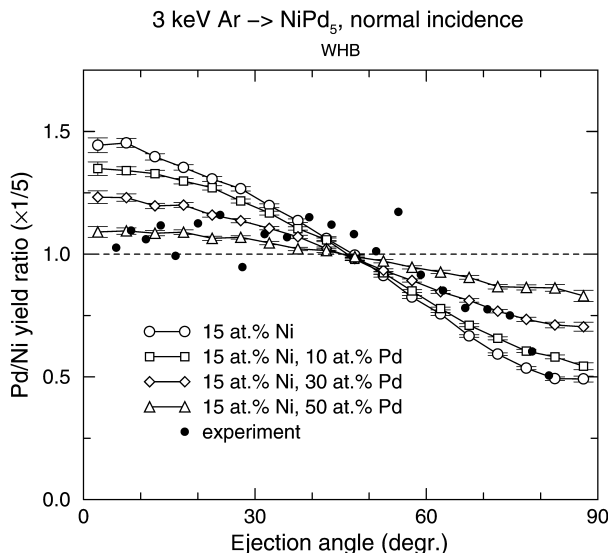


Figure 4. Same as Figure 3 (c) for various concentrations of segregating atoms.

in the bulk of the target ($C_{Pd}/C_{Ni} = 5$). It is seen that such a 'bulk' combination of the surface Ni and Pd atoms is completely inadequate in explaining the experimental data.

It should be noted that a good description of the NiPd₅ experimental data can be also reached at $S_{Ni} > 10$ at.% and nonzero values of S_{Pd} , for example at $S_{Ni} = 15$ at.% and $S_{Pd} \sim 30$ at.% (Figure 4). The corresponding best-fit value of the ratio $S_{Pd}/S_{Ni} < 5$, which again is indicative of surface segregation of Ni.

5. Conclusions

For a Ni₅Pd alloy, a reversion of atomic segregation was observed (3) in going from sputtering with noble gas ions (argon) to sputtering with reactive ions (oxygen). The results of the present work demonstrate that such a reversion is also possible at low initial concentrations of one of the components.

References

- (1) Betz, G.; Wehner, G.K. In *Sputtering by Particle Bombardment II*; Behrisch, R., Ed.; Springer: Berlin, *Top. Appl. Phys.* **1983**, 52, 11.
- (2) Andersen, H.H.; Chernysh, V.S.; Stenum, B. et al. *Surf. Sci.* **1982**, 123, 39.
- (3) Andersen, H.H.; Stenum, B.; Sorensen, T. et al. *Nucl. Instrum. Methods B* **1983**, 209/210, 487.
- (4) Chernysh, V.S.; Kulikauskas, V.S.; Patrakeev, A.S. et al. *Radiat. Eff. Def. Sol.* **2004**, 159, 149.
- (5) Shulga, V.I. *Radiat. Eff.* **1983**, 70, 65.
- (6) Eckstein, W. *Computer Simulation of Ion-Solid Interactions*; Springer: Berlin, 1991.
- (7) Shulga, V.I. *Nucl. Instrum. Methods B* **2007**, 254, 200.
- (8) Ziegler, J.F.; Biersack, J.P.; Littmark, V. *The Stopping and Range of Ions in Solids*; Vol.1, Pergamon: New York, 1985.
- (9) Eckstein, W.; Hou, M.; Shulga, V.I. *Nucl. Instrum. Methods B* **1996**, 119, 477.
- (10) Shulga, V.I.; Sigmund, P. *Nucl. Instrum. Methods B* **1996**, 119, 359.
- (11) Shulga, V.I.; Eckstein, W. *Nucl. Instrum. Methods B* **1998**, 145, 492.
- (12) Sigmund, P. *Nucl. Instrum. Methods B* **1987**, 27, 1.